# A Customizable Fitting Protocol for the Body-Machine Interface

Fiona A. Neylon[1,2], Andrew Thompson[1,2], Rachel Kalvakota[2],
Corinne Fischer[2], Fabio Rizzoglio[1,2], Lee Miller[1,2], and Brenna D. Argall[1,2]

***Abstract*— In this work, we present a case study evaluation that compares two methods of fitting the Body-Machine Interface (BoMI) to an individual with cervical spinal cord injury for the purpose of operating a robotic arm in 6-D. A BoMI is a control interface created by recording body movements and mapping them to the controls of a device or machine, and has shown promise for individuals with motor impairments whose access to standard interfaces is otherwise limited. Results from this case study show a one-size-fits-all placement strategy is not a sufficient fitting method for an individual with severe upper extremity limitations. However, when a flexible fitting protocol informed by a clinical evaluation is applied, we see improvement in two key categories: (1) success in map fitting and (2) robot task results. Informed by the case study analyses, we develop a *novel* method to customize and fit the BoMI to users in a way that is analogous to how commonly used assistive technologies are fit clinically: the BoMI Customization Evaluation (BCE). This new method of customization is determined from a physical evaluation conducted by a clinician in conjunction with participant feedback and BoMI engineers. Deployment of this novel method within a full evaluation study is underway. The current work focuses on the evolution to this protocol.**

## I. Introduction

Individuals living with cervical spinal cord injury (cSCI) depend on a variety of assistive technologies to perform activities of daily living (ADL). The commonly used powered wheelchair employs low-dimensional control (2-D) to achieve increased mobility [1]. The less commonly used robotic arm requires high-dimensional control (e.g., 6-D) to assist those with upper extremity limitations with feeding, picking-and-placing objects, or opening doors [2].

For those with cSCI, their assistive technologies (ATs) are not traditionally out-of-the-box ready. Users undergo fittings, calibrations, and customization options with clinicians. For a powered wheelchair, components of the chair such as seating interfaces, suspension mechanisms, and driving interfaces are written into a prescription [3]. For a sip/puff interface, the user undergoes a calibration protocol to construct a mapping from their respiration pressure signals to device controls. However, to the knowledge of the authors, an analogous prescriptive fitting protocol informed by clinical metrics does not exist for the Body-Machine Interface (BoMI).

We address this gap by designing the BoMI Customization Evaluation (BCE)—a prescriptive fitting protocol for the BoMI. A BoMI is a control interface created by recording body movements and mapping them to the controls of a device or machine. It has shown promise for individuals with motor impairments whose access to standard interfaces is otherwise limited [4]. We motivate the final BCE design through a case study evaluation of two BoMI fitting protocols, in which an individual with cSCI operates a robotic arm in 6-D. The contributions of this work are the following:

- A case study evaluation of two evolutions of BoMI fitting protocols to a person with cSCI for the purpose of robotic arm operation.
- The identification of a collection of considerations and guidelines when fitting wearable interfaces, such as the BoMI, to individuals with cSCI.
- A prescriptive fitting protocol for a BoMI to persons with upper-extremity mobility limitations: the BoMI Customization Evaluation (BCE).

In Section II, we present related background and describe the current gap in BoMI fitting protocol. We then present the evolution of our three approaches to fitting the BoMI in Section III. We setup our case study experimental protocol and evaluation metrics in Section IV and discuss the results in Section V. We summarize our takeaways and future work in Sections VI and VII.

## II. Background & Related Work

For people both with and without injury, the use of interfaces to send a control signal to a device is a daily phenomenon; even pressing a button for an elevator is an example of a control interface. For those with cSCI and resultant upper and lower extremity impairments, the dependence on control interfaces is more significant. The interfaces accessible to them vary in operation, type, and issued signal depending on their injury level.

Common non-invasive interfaces used by cSCI individuals include joysticks, head arrays, sip/puffs (SNPs), and micro light switches (MLSs) [5]. The joystick, at most a 3-D interface, becomes limited or completely inaccessible to those with severe paralysis. Alternatives such as head arrays (2-D), SNPs (1-D), and MLSs (1-D) issue even lower dimensional signals. Moreover, when using traditional interfaces for higher-dimensional control, such as a robotic arm (6-D), there is a dimensionality mismatch between the issued signals and the device's control space.

One solution to this mismatch is the use of *modal control*—the partitioning of the control space into subsets, with *mode-switch* actions that change the operational mode of the interface in order to access the various subsets [6]. The added hurdle of mode switching can increase the mental and physical load on the user, and accordingly also the difficulty of simple ADL tasks [7].

[1]Northwestern University, Evanston, IL., USA
[2]Shirley Ryan AbilityLab, Chicago, IL., USA

A challenge when designing and fitting ATs to people with cSCI is how the same injury can manifest as very different movement capabilities [8], lending customization to be a desired feature. The aforementioned interfaces are commercially available in part due to their limited customization options. For the joystick, handle interfaces can be changed—for example to a T-bar for high cSCI individuals—but this modification reduces the input space from 3-D to 2-D. Moreover, any 1-D or 2-D interface requires significant mode switching when controlling high-dimensional devices—furthering the cognitive load.

The BoMI provides an alternative solution to address the dimensionality mismatch between ATs and their control interfaces, while maintaining the capability of customization to meet users where *they* are physically. The BoMI uses sensors to capture and translate body motions to control signals; common methods include capturing body kinematics via Inertial Measurement Units (IMUs) or cameras, and muscle signals via electromyography [4], [9], [10]. There is preliminary evidence that BoMIs are able to issue sufficiently high control signals to obviate the need for mode switching during robotic arm operation [11].

## III. Body-Machine Interface Fitting

We present in this section an evolution of three BoMI fitting methods. In Method 1 (Sec. III-A), customization of the BoMI focuses on sensor placement and selection from a menu of vetted motion prompts. *Motion prompts* are body motions that are collected during calibration to obtain the parameters of the BoMI map, and which will be executed to operate the robotic arm. Method 2 (Sec. III-B) is a flexible approach, fitting the sensors and prompts based on the movement capabilities of the participant.

A case study comparison of these two methods then drives the development the third method. Method 3 (Sec. III-C) is a prescriptive approach which combines input from three parties—clinicians, BoMI engineers, and the user—in a collaborative effort to customize the BoMI.

Our target population is individuals with cSCI with a complete (ASIA A) lesion at C3-6 or an incomplete injury (ASIA B, C, or D) lesion in the cervical cord. These are individuals who have limitations in hand and manipulation ability, but also the potential to execute six distinct upper-body movements: that is, individuals who would benefit from the use of an assistive robotic arm, and would potentially be able to operate it without mode switching.

### A. Method 1: Fixed Procedure

Method 1 fits a predetermined configuration of prompts and sensor placements to a user. As a default, the shoulder (up/down and forwards/backwards) and arm (elbow abduction/adduction) prompts are paired with empirically determined sensor placements limited to the shoulders (front/back) and arms (upper/fore). These default prompts are chosen as upper body joint motions that our target population are expected to be able to perform [12].

With the user in their seated rest position, we record a dataset as they execute the motion prompts. If the user is unable to reproduce a prompt, we replace it with a head prompt—defined as head up/down, left/right, up-right(UR)/down-left(DL), up-left(UL)/down-right(DR), or tilt right/left. These configurations are hypothesized to decrease the likelihood of generating an invalid map—a map wherein the user does not have access to all the required control dimensions.

### B. Method 2: Flexible Procedure

Method 2 takes a flexible fitting approach to the BoMI that does not use a default configuration; instead, the configuration is defined via the range of motion (ROM) of the user. The user undergoes a clinical evaluation which assesses areas of the body to define the ROM. The results inform a fitting with the user, clinicians, and experimenters.

The user is asked to perform common upper extremity (UE) motions that they are expected to have access to based on the results of the ROM exam. Experimenters select six visually distinct movements—with visually appreciable motion and with limited similarity. Formally, these are motions in which extremities follow a rotation around orthogonal axes bisecting a common joint, which allow for conscious isolation between the six motions during execution. IMUs then are fit to the user's UEs with placements able to record the selected prompts.

### C. Method 3: BoMI Customization Evaluation (BCE)

Method 3, the prescriptive approach, comprises two phases: (1) physical examination and (2) collaborative fitting.

**Physical Examination.** The first phase is comprised of a clinical evaluation protocol plus an evaluation framework that categorizes cervical and UE movements based on potential sensor placements. This evaluation framework ultimately facilitates the identification of viable sensor placements and the assessment of the movement quality at each placement.

Clinical Protocol. The clinical evaluation incorporates measurements of UE active range of motion (AROM) and utilizes a modified version of the International Standards for Neurological Classification of Spinal Cord Injury (ISNCSCI) [12] in an effort to provide insights into the users' residual motor abilities. The ISNCSCI provides an objective framework to quantify injury levels, thereby facilitating consistent comparisons among users. To enhance user comfort and minimize unnecessary procedures, modifications are made to the ISNCSCI, substituting the anal testing component with a self-report questionnaire [13]. This study targets individuals with injuries at or above the C8 level, so the sensory assessment concludes at T2, while the motor assessment is unaltered.

Movement Categorization. The movement scoring framework begins with a Manual Muscle Test (MMT) to the cervical and bilateral UE regions, reflective of any movement eligible for IMU placement. Unlike the MMT scale used in the ISNCSCI, the 5-point MMT scale used is a variation that is more sensitive to lower strength levels, which is relevant data when selecting optimal sensor placement [14]. This scale defines 0 as having no muscle contraction and 5 as normal muscle contraction with full motion in a gravity plane against maximum resistance. A score of 2 on the ISNCSCI

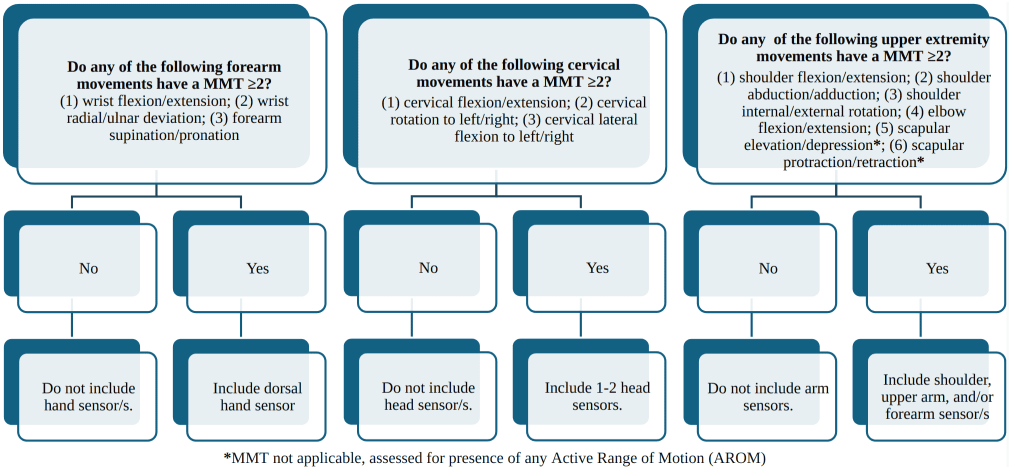


**Fig. 1:** Flowchart directing the sensor placement based on the movement score in each region.

MMT rubric requires full ROM in a gravity-eliminated plane, while a score of 2 on the updated scale only requires some motion. This provides a more nuanced scoring for someone who does not have full ROM, typical of our target population.

The MMT motions are divided into categories based on sensor placement, presented in Figure 1. For example, the eligibility of a hand sensor placement is determined by evaluating wrist flexion/extension, radial/ulnar deviation, and forearm supination/pronation. If the MMT score is 2 or greater for any movement in the sensor category, it qualifies as a valid sensor placement.

**Collaborative Fitting.** In the second phase, the clinician presents the list of valid sensor locations and the corresponding movements with above-threshold MMT scores. The BoMI developers choose six visually distinct movements: with appreciable motion and limited similarity (as in Section III-B). Experimenters ask the user to execute the prompts and visually inspect if appreciable motion is achieved on their body. The user then is asked if these prompts are comfortable and non-strenuous. If the user responds 'no', the prompt is either swapped out for an alternative high-scoring motion prompt in the same region, or the user may alter the execution of the motion to be within their comfort level. Once the motions are finalized, developers pre-assign each prompt to a specific robot control dimension.

## IV. Experimental Protocol

Here we overview the experimental protocol for case study evaluations of BoMI fitting Methods 1 and 2, the results of which motivate the creation of the BCE.

### A. Participant Profile

We compare Methods 1 and 2 with respect to BoMI fitting and operation by a 68 year-old male with a self-reported cSCI injury level at C2. The onset of injury was approximately 4 years ago after suffering from a spinal stroke post heart attack. Since his diagnosis, he uses a powered wheelchair daily controlled by a T-bar joystick, and self-assesses being 'comfortable' controlling his device. Participant also self-assesses experience controlling a wheelchair with a head array, but 'not experienced' controlling a robotic arm. The participant gave his informed, signed consent to participate in the experiment which was approved by the Northwestern University Institutional Review Board.

### B. Hardware & Software

The experimental BoMI consists of 6 IMU sensors that capture body motions predefined according to the fitting procedure (Method 1 or 2). The 24-D quaternion signals issued from the IMUs ($\mathbf{q}_{[1\times 24]}$) are mapped via supervised learning to a 6-D robot end-effector control space ($\mathbf{v}_{[1\times 6]} = [\dot{x}, \dot{y}, \dot{z}, \dot{\phi}_x, \dot{\phi}_y, \dot{\phi}_z]$).

Specifically, a k-nearest neighbors classifier ($k = 50$) is used to predict the probability of each of the pre-selected prompts ($\Gamma^{[1\times 6]}$) given the user's movement as captured by the IMUs (Algorithm 1). The robot control dimension associated with the most likely prompt is selected for execution. The magnitude of the robot motion is determined from Principal Component Analysis (PCA) maps derived *a priori* for each of the 6 prompts from the calibration data ($\mathscr{D}$, described in Section IV-D); the first principal axis of the associated PCA map is used to determine the amplitude of the control signal for the selected control dimension.

The IMUs are the x-io Technologies x-IMU3 (Bristol, UK). The robotic arm is the 7-DoF UFactory xArm7 (Shenzhen, China) with associated ROS2 Humble packages. The experimental pipeline runs on a Lenovo ThinkStation P3 Tower (64GB RAM, 13th Gen Intel$^{TM}$ Core i9-1300 x32 processor) running Ubuntu 22.04. Hardware is commanded and data is logged using Open Robotics ROS2 Humble.

### C. Data Collection

From fitting Method 1, we construct Configuration $C_1$ (Figure 2). Sensor placements are front of the shoulders (1/2), upper arms (3/4), and sides of the head (5/6). The prompts and map to robot controls for $C_1$ are: (1) Head R/L $\rightarrow x$, (2) R shoulder forwards/backwards $\rightarrow y$, (3) R shoulder up/down $\rightarrow z$, (4) L shoulder up/down $\rightarrow \phi_x$, (5) Head up/down $\rightarrow \phi_y$, and (6) L shoulder forwards/backwards $\rightarrow \phi_z$.

From Method 2, we construct configuration $C_2$ (Figure 2). Sensor placements for this configuration are front of the

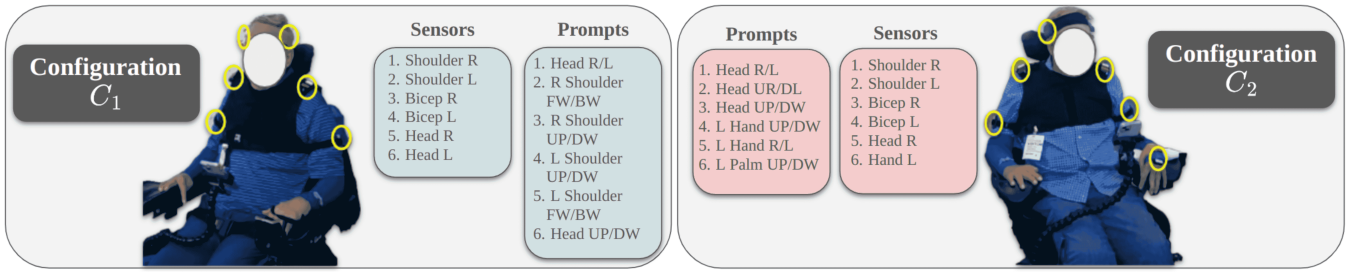


**Fig. 2:** Experimental setup showing the prompts and sensor placements for configuration 1 ($C_1$) and configuration 2 ($C_2$)

**Algorithm 1** BoMI Mapping Using KNN and PCA

**Input:** 24-D quaternion input $\mathbf{q}^{[1\times 24]}$ and $\mathscr{D}$
**Ouput:** 6-D control signal $\mathbf{v}^{[1\times 6]}$
**Step 1: Calibration (Offline)**
**for** each motion prompt $\gamma_i \in \Gamma^{[1\times 6]}$ **do**
Derive PCA map $\mathbf{PCA}_i$ from $\mathscr{D}_i$
**end for**
**Step 2: Motion Prediction (Run-time)**
Use $k$-nearest neighbors (KNN, $k = 50$) to predict the probability vector

$$\mathbf{p} = \mathrm{KNN}(\mathbf{q}) \quad \text{where } \mathbf{p} \in [0,1]^{1\times 6}$$

Identify Highest Probability Index

$$i^* = \arg\max_i p_i$$

**Step 3: Compute Velocity Vector (Run-time)**
Reduce the 24-D signal to 1-D using the first principal axis of $\mathbf{PCA}_{i^*}$:

$$a = \mathbf{q} \cdot \mathbf{PCA}_{i^*,1}$$

Compute the final control signal:

$$\mathbf{v} = [0,\ldots,a,\ldots,0]$$
$$\uparrow$$
$$i^*\text{th position}$$

shoulders (1/2), upper arms (3/4), side of the head (5), and top of the left hand (6). The prompts and map to robot controls for $C_2$ are: (1) Head R/L $\rightarrow x$, (2) Head UR/DL $\rightarrow y$, (3) head up/down $\rightarrow z$, (4) L hand up/down $\rightarrow \phi_x$, (5) L palm up/down $\rightarrow \phi_y$, and (6) L hand right/left $\rightarrow \phi_z$.

For this analysis, we focus on 4 study sessions: 3 sessions under $C_1$ ($C_1^{S_1}$, $C_1^{S_2}$, and $C_1^{S_3}$) and 1 session under $C_2$ ($C_2^{S_1}$), which define the divide between the two different fitting protocols. We focus on these sessions to highlight the immediate effects of changing to a BoMI configuration informed by a clinical evaluation. For the three $C_1$ sessions, each session occurred within 4 days of each other. The $C_2$ session occurred 16 days later. This is due to the presence of 3 *wash* sessions (defined in Section IV-E) that occurred under the $C_1$ fitting method, in which the $C_1$ map became unusable as a result of physiological changes in the participant—specifically, reduced ROM due to a gap in physical therapy.

### D. Calibration

Each session begins with a calibration phase. The participant executes directed motion prompts to generate the dataset $\mathscr{D}$ for map computation. This is done in a cyclic fashion, where each prompt is executed in sequence 6 times. A sequential approach, in comparison to repeated iterations, is expected to better reflect the control signals the user issues during teleoperation, and also to mitigate the biased accumulation of IMU drift across the recording (sampling at 50Hz).

### E. 6-D GUI Validation

Next, a 6-D GUI task is used to validate the map—ensuring that the participant has isolated control of each of the required dimensions (Figure 3a). The GUI is a circular figure divided into 6 equally spaced wedges with a different color arc located in the center of the wedge [15]. Each arc begins in a grey zone of the wedge which defines the *deadzone* of the control space that maps to the bodily rest position of the user. The colored arc moves in accordance to the magnitude of the velocity control signal issued by the user and returns to the *deadzone* when no signal is being issued.

To validate, the experimenter instructs the participant to execute a body prompt. If the correct arc displaces in the correct direction, the signal is considered valid. A valid map is defined as the user being able to issue intended and correct signals using the defined body motions in both the positive and negative directions for the required control dimensions, defined at a minimum to be 3-D translation. This is conducted for all 6 prompts in each direction (+/-), for 12 distinct movements total.

Wash Sessions. If instead a direction is considered invalid—incorrect or with no activation after repeated attempts—we *tare* the BoMI: the participant returns to their self-defined rest position, and we tare the IMU quaternions back to zero to eliminate any drift accumulation that might have caused poor GUI performance. We then revisit the invalid directions and ask the participant to repeat the motion.

If the map is deemed invalid—incorrect or no activation after repeated attempts in one or more of the required control dimensions—the most recent valid map (from prior sessions) is tested under the same protocol. If this map is valid, it is used, otherwise the calibration protocol is executed again. If the re-recorded map results in an invalid map, the session is a *wash* and concludes without progressing further.

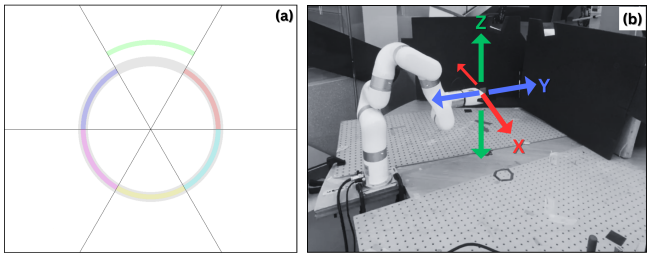


**Fig. 3:** Experimental setup where (a) shows the 6-D GUI validation task and (b) shows the 3-D Dimensional Freezing task.

### *F. 3-D Dimensional Freezing (DF)*

The 3-D Dimensional Freezing (DF) task is a training task to teach users to command the robotic arm with the BoMI. For each translation dimension, the user practices how to independently move the robot end-effector in one dimension at a time in a center-out-reaching fashion (Figure 3a). During these reaches, the robot motion is restricted to only move in the training dimension, effectively filtering out all spurious BoMI commands and allowing only those that achieve motion in the intended robot dimension to pass through. We ask the participant to complete 3 reaches in a row for each robot control dimension.

### *G. Metrics*

Expert Comparison. A common method used to evaluate reaching tasks is to define an 'expert' or desired trajectory and compare reaching trials [16]. To analyze the DF trials, we define an expert trajectory for each center-out reaching translation dimension. This expert trajectory is defined as a time series of end-effector positions as a result of a synthetic velocity control signal roll-out on the robot. For all trajectories, a moving window average ($N = 10$) is used to filter out mechanical noise from the profile of the end-effector positions, sampled at 100 Hz.

We use Dynamic Time Warping (DTW) to quantify the similarity between the participant trajectories and the expert trajectory. DTW lends itself to being useful for comparing time series profiles where events occur during a window of time—this algorithm has been used to compare trajectories [17]. We use the Fast Distance Dynamic Time Warping method from the DTAIDistance Python package [18].

Trajectory Characteristics. We also examine a number of *trajectory characteristics*. Three main characteristics we look for in a reach are, relative to the end-effector start position, (1) the presence of a departure path due to a positive velocity signal, (2) a turnaround, and (3) a return path due to a negative velocity signal. The presence of each indicate the user, at a rudimentary level, is able to not only access all areas of the control space for that dimension, but is also able to purposefully elicit the correct sequence of commands that would allow them to complete the task as asked.

We construct a scoring paradigm that looks for this sequence of events, or partial sequence at any point during the reach. We assign a score of 1 if the characteristic: (1) is present, (2) in the correct direction, and (3) occurs in the proper sequence of events (departure→turnaround→return).

**TABLE I:** Summary of trajectory characteristics.

| | Characteristic | $C_1^{S_1} - C_1^{S_3}$ | $C_2^{S_1}$ |
|---|---|---|---|
| **X Reaches** | *Departure* | 3.0 ± 0.0 | 3.0 |
| | *Turn around* | 3.0 ± 0.0 | 3.0 |
| | *Return* | 3.0 ± 0.0 | 3.0 |
| **Y Reaches** | *Departure* | 1.7 ± 1.2 | 3.0 |
| | *Turn around* | 1.3 ± 1.2 | 2.0 |
| | *Return* | 1.0 ± 0.8 | 2.0 |
| **Z Reaches** | *Departure* | 2.3 ± 0.9 | 3.0 |
| | *Turn around* | 2.0 ± 0.8 | 3.0 |
| | *Return* | 1.0 ± 0.8 | 3.0 |

The characteristic otherwise is assigned a score of 0.

Cross-talk. We finally look to the raw signals issued by the user during teleoperation. For every set of dimensional reaches and each timestep of each reach, we count the commands issued in every control dimension. This is to analyze *cross-talk*—in which unintended control dimensions are accessed due to prompt similarity.

With limited mobility, there are limited body sites to choose from for the motion prompts. When a single mobility site needs to be overloaded with multiple distinct motion prompts, the possibility of *cross-talk* is present. This introduces an optimization problem when fitting the BoMI, wherein we choose sites to maximize movement activation while minimizing crosstalk between prompts. An example of *cross-talk* would be if a third motion prompt combines two motion prompts off-axis (e.g., head up/down, left/right, and up-right/down-left). Within the latent space of the map, the user might have to pass through a region of one of the first two prompts before reaching the more defined and separated area of the third prompt, and within this region inadvertent commands would be issued.

Map & Experimental Metadata. In addition to robot task data, map and experimental metadata is considered to assess how reliable the fit is between days. We measure this by calculating (1) the percentage of wash sessions across all sessions, (2) the average number of calibration recordings per session, and (3) the number of modifications along with the intensity of the modification.

## V. Results

We present the results of the metrics described in Section IV-G; this includes results from the 3-D DF task and metadata from the maps collected over the sessions.

### *A. Robot Task Results*

Trajectory Characteristics. Table I summarizes the breakdown of the presence of each trajectory characteristic during each session. The end-effector trajectories for the corresponding reaches are shown in Figure 4.

Comparing the two fitting protocols, the $y$ reaches improve by greater than 50% under $C_2$; notably, none of the characteristics are present in $C_1^{S_3}$. In $z$ under $C_1$ the participant has difficulty obtaining a turn-around or return path; for these

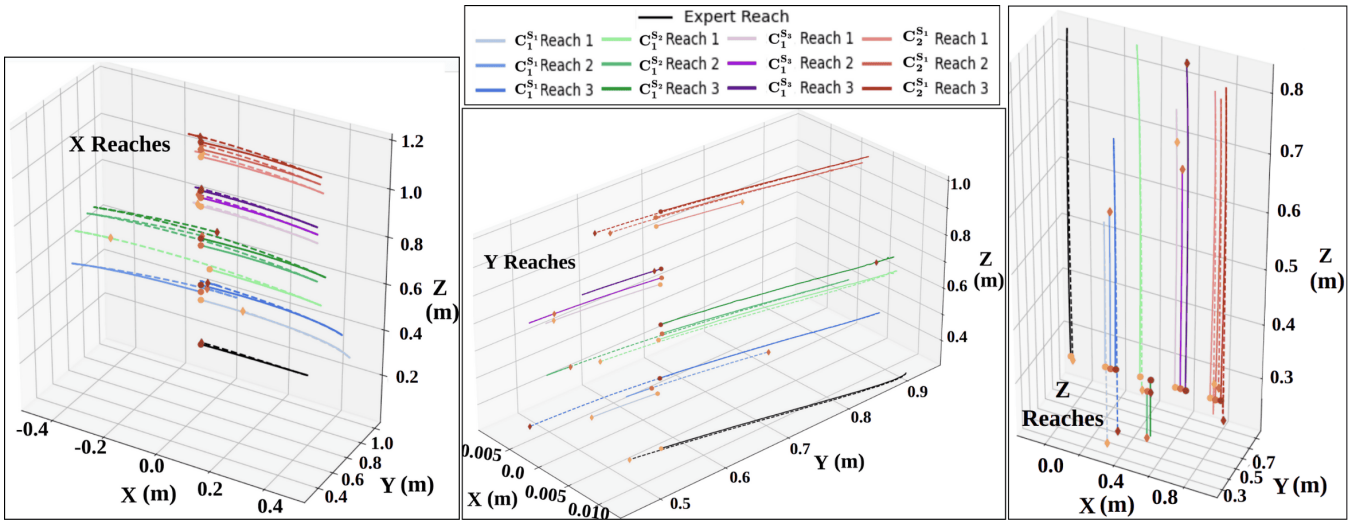


**Fig. 4:** Comparison of robot end-effector positions for $C_1^{S_1}$-$C_1^{S_3}$ and $C_2^{S_1}$. Reaches under $C_1$ are blue/green/purple, and under $C_2$ are red, with the expert trajectory in black. Motion prior to the first turnaround is presented as solid lines, and post turnaround as dashed lines. Start (yellow circle) and end (yellow diamond) positions indicated for each trajectory. Reaches are offset for visibility: by 0.03m within a single session, and by 0.2m between sessions.

two characteristics, there is greater than 130% increase with $C_2$. By contrast, for the $x$ reaches (unchanged dimension), the presence of these characteristics is stable across all sessions and configurations.

Expert Comparison. In Figure 5, we see the mean DTW distance for each type of dimensional reach between $C_1$ and $C_2$. Comparing the two changed dimensions, $y$ and $z$, there is an immediate ∼45% reduction in the DTW distance for each dimension ($5.30 \pm 1.02$m to $2.84 \pm 0.55$m for $y$, and $8.93 \pm 1.44$m to $5.04 \pm 0.21$m for $z$) following the configuration change, $C_1^{S_3}$ and $C_2^{S_1}$.

While not statistically significant (Wilcoxon non-parametric statistical t-test), these reductions do indicate that the changes in configuration positively impacted robot operation performance. In the $z$ dimension, performance under $C_1$ progressively erodes across sessions, while performance in the $y$ dimension is consistently inferior to that under $C_2$. All sessions under $C_1$ furthermore display higher variability than $C_2$, in both dimensions $y$ and $z$.

By contrast, for the unchanged $x$ dimension, the DTW averages were comparatively similar between $C_1$ and $C_2$

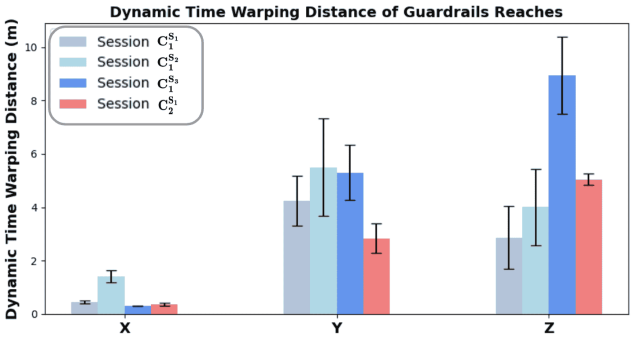


**Fig. 5:** Average DTW distance computed across reaches for $C_1^{S_1}$-$C_1^{S_3}$ and the $C_2^{S_1}$. The blue-toned bars indicate sessions under $C_1$ and the red-toned bars indicate sessions under $C_2$.

($0.31 \pm 0.01$m and $0.38 \pm 0.06$m, respectively), and are smaller overall. These results underline the suitability of the BoMI motion prompt affiliated with $x$ dimension robot control, and also confirm that the change from $C_1$ to $C_2$ did not impact the operability of this motion prompt.

For $C_2$ we also see the average distance traversed is comparatively closer to the expert reach, in each of dimensions $x$ (expert: 0.79m, $C_2$ : $0.97 \pm 0.08$m, $C_1$: $1.23 \pm 0.32$m), $y$ (expert: 0.74m, $C_2$ : $0.45 \pm 0.24$m, $C_1$: $0.38 \pm 0.25$m), and $z$ (expert: 1.15m, $C_2$ : $1.15 \pm 0.08$m $C_1$: $0.54 \pm 0.34$m).

Cross-talk. In Figure 6, we compare the commands issued under configurations $C_1^{S_3}$ and $C_2^{S_1}$. Specifically, for each intended control dimension, we tally the number of (positive/negative) commands issued all control dimensions.

We see for $C_2$, there is more *cross-talk*. This is not surprising with $C_2$ because the body prompt for $y$ activation (head UR/DL) is a combination of the body prompts for $x$ (head R/L) and $z$ (head UP/DW). The user therefore likely needed to pass through a latent space region corresponding to $x$ or $z$ to reach $y$ area. The body, specifically the upper body, is highly coupled which means that *cross-talk* (between prompts and, accordingly, control signals) is a natural feature of the BoMI that users need to learn how to manage.

We also, however, see more correct $y$ and $z$ signals issued under C2. These signals additionally are more balanced in the ratio of positive to negative signals, indicating reliable access to dimensions in both the positive and negative directions.

### *B. Map & Experimental Metadata*

Our analysis so far has focused on 4 study sessions, to dive deep into the impact of the configuration change from $C_1 \rightarrow C_2$. We now zoom out for a moment, and examine metadata from all sessions with this participant, including *wash* sessions and continued sessions with $C_2$. The total number of sessions is 17: 8 under $C_1$ and 9 under $C_2$.

Wash Sessions. Looking at all of the maps recorded over all

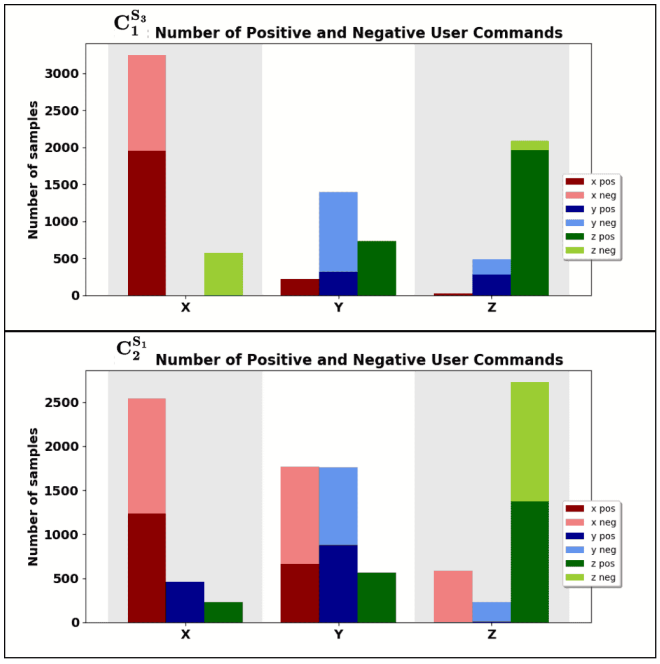


**Fig. 6:** Comparison of user signals commanded under $C_1$ and $C_2$. More *cross-talk* between dimensions is evident in $C_2^{S_1}$ than $C_1^{S_3}$, however the signals in $y$ and $z$ also are more correct and more balanced. (No crosstalk would have only a red bar in $x$, only a blue in $y$, and only a green in $z$.)

17 attempted sessions, for each configuration two metrics are calculated: (1) percentage of wash sessions of the attempted sessions and (2) average number of maps recorded per session. With $C_1$ we see 37.5% of the attempted sessions end in a *wash* protocol; for $C_2$ that number is 0.0%. The number of recorded maps per session is reduced from an average of 1.9 recordings per session to 1.1 recordings per session. Both of these metrics signal an informed approach to fitting the BoMI results in a more reliable mapping mechanism that is more robust to day-to-day variation. This not only eases the burden on experimenters and clinicians, but also on the user.

Moreover, while the evaluation of the BCE protocol is beyond the scope of this paper, we note that it has since been deployed in a total of 67 sessions across 8 participants, *none* of which has ended in a *wash* session.

Modifications. It is expected that unforeseen modifications will need to be made to the BoMI between users, as modifications made to ATs are not uncommon in the field [19]. Between $C_1$ and $C_2$, the physical and environmental modifications made in order to get the BoMI to work on a given day changed, including number and type.

Across all 17 sessions, we catalog 3 types of modifications: (1) removing wheelchair armrests, (2) providing limb support, and (3) restraining limbs. If the same type of modification is applied to both sides of the body, we count it as 2 modifications.

For $C_1$, 4 modifications were applied: (1/2) removing right/left armrest, and (3/4) restraining the right/left arm to wheelchair armrest. There was also a lack of consistency in whether a modification actually resulted in any appreciable difference in the map validity. In comparison, the only modification for $C_2$ during the 9 attempted sessions was the support of the left wrist to elevate the hand. This modification not only was less invasive compared with modifications made in $C_1$, but also was applied to every session as it positively impacted map validity.

## VI. Discussion

For this work, we consider both the quantitative robot task data and the map metadata to provide insights into assessing the fit of each configuration (Section VI-A). We also compile our observations from this case study into guidelines for those working with wearable interfaces similar to the BoMI on individuals with cSCI (Section VI-B). Our on-going and future work will continue to evaluate the BCE, in a multi-session user study with the cSCI population.

### A. Quantitative Results

This case study marks a milestone in the experimental development for properly fitting the BoMI. When trying to implement Method 1 on an AROM-restricted participant, the interface was unreliable and, at times, completely unusable. Once we took a flexible approach with Method 2, we not only saw *immediate* improvement in the day-to-day fitting and calibration process, but we also saw improvement in robot task performance. The inconsistencies and low yield of desired characteristics in the $y$ and $z$ dimensions in the DF task improved immediately in the first session with $C_2$.

It is suspected that motor learning of the interface was not the cause of this improved performance: in Figure 5, $C_1^{S_1} \rightarrow C_1^{S_3}$ in fact was moving farther away from the expert trajectory, prior to the switch to $C_2$. The lack of statistical significance in these results is hypothesized to be due to a small sample size ($N = 3$). Finally, the consistent trajectory characteristics across the $x$ reaches indicated the $x$ dimension was properly fitted from the beginning.

### B. cSCI Wearable Considerations

The AT field expects modifications to fully meet the user. The reliability of these modifications requires an open dialog between clinicians, developers, and the user. The flexibility built into our mapping paradigm, taring protocol, and choice of hardware are vital to meeting these needs. The mapping paradigm has parameters, such as *deadzone* size, to algorithmically tune the sensitivity per participant. The taring protocol is the key to combating drift accumulation in the IMUs, which becomes even more vital when working with the relatively low-variance samples enacted by lower-ROM movements. The use of appropriate hardware and filtering methods enables the capture of these low-variance signals, in turn allowing for accurate mapping. These three components introduce robustness into a system that interfaces with a population with high physiological variability.

The need for stability in the user/device relationship is all the more pressing when any physical instability will manifest in the interface; because the stability of a wearable interface is tied to the stability of the user's body. Creating a system that is robust to instabilities results in a more learnable system by minimizing stochastic components of the user map. For example, our cSCI population requires

frequent pressure breaks and additional personal needs that cause changes in the position of the IMU and overall postural positioning. The user should be able to do these things, re-tare the interface, and resume operation as normal. Artifacts such as *cross-talk*, a present and unavoidable consequence of working with a population with limited sites for appropriate sensor placement, becomes more predictable and learnable to the user when the system is reliable and robust.

## VII. Conclusions

The value of designing ATs that are inherently customizable lies in their ability to meet the diverse needs of individuals with varied motor abilities. Traditional interfaces to control ATs often fail to address the full spectrum of user needs due to their fixed design, which limits adaptability and accessibility. We have presented an evolution of protocols that fit a Body-Machine Interface (BoMI) to a person with cervical spinal cord injury (cSCI) for the purpose of 6-D robotic arm control. A case study comparison of the first two protocols has demonstrated the benefit of introducing flexibility into the fitting protocol, with improvements in the day-to-day fitting and calibration process as well as in robot task performance. We also have introduced the BoMI Customization Evaluation (BCE): a user-centric fitting approach that includes a clinical evaluation and combines input from three parties—clinicians, BoMI developers, and the user—in a collaborative effort to customize the BoMI to ensure that both the clinical and functional requirements of the technology are met. The evaluation of the BCE within a multi-session study with cSCI users is on-going, with promising preliminary results.

## Acknowledgments

The authors would like to thank Lucy Ammon and Divyanka Thakur for their assistance in running study sessions and data analysis. Funding for this work was provided by the National Institute of Biomedical Imaging and Bioengineering (NIBIB) under Award Number R01-EB024058. The content is solely the responsibility of the authors and does not necessarily represent the official views of the NIH.

## References

[1] J. Florio, U. Arnet, A. Gemperli, T. Hinrichs, and SwiSCI study group, "Need and use of assistive devices for personal mobility by individuals with spinal cord injury," *Journal of Spinal Cord Medicine*, vol. 39, no. 4, pp. 461–470, 2016.

[2] V. Maheu, P. S. Archambault, J. Frappier, and F. Routhier, "Evaluation of the jaco robotic arm: Clinico-economic study for powered wheelchair users with upper-extremity disabilities," in *Proceedings of the IEEE International Conference on Rehabilitation Robotics (ICORR)*, 2011.

[3] E. Michael, T. Sytsma, and R. E. Cowan, "A primary care provider's guide to wheelchair prescription for persons with spinal cord injury," *Topics in Spinal Cord Injury Rehabilitation*, vol. 26, no. 2, pp. 100–107, 2020.

[4] M. Casadio, R. Ranganathan, and F. A. Mussa-Ivaldi, "The body-machine interface: a new perspective on an old theme," *Journal of Motor Behavior*, vol. 44, no. 6, pp. 419–433, 2012.

[5] K. Cezat, "Power wheelchair alternative drive controls in spinal cord injury," 2019.

[6] J. D. Simon and S. K. Mitter, "A theory of modal control," *Information and Control*, vol. 13, p. 316–353, 1968.

[7] H. Tijsma, F. Liefhebber, and J. Herder, "A framework of interface improvements for designing new user interfaces for the manus robot arm," in *Proceedings of IEEE International Conference on Rehabilitation Robotics (ICORR)*, 2005.

[8] R. Parasuraman and V. Riley, "Humans and automation: Use, misuse, disuse, abuse," *Human Factors*, vol. 39, no. 2, p. 230–253, 1997.

[9] M. MacChini, F. Schiano, and D. Floreano, "Personalized telerobotics by fast machine learning of body-machine interfaces," *IEEE Robotics and Automation Letters*, vol. 5, no. 1, pp. 179–186, 2020.

[10] E. B. Thorp, F. Abdollahi, D. Chen, A. Farshchiansadegh, M.-H. Lee, J. P. Pedersen, C. Pierella, E. J. Roth, I. S. Gonzales, and F. A. Mussa-Ivaldi, "Upper body-based power wheelchair control interface for individuals with tetraplegia," *IEEE Transactions on Neural Systems and Rehabilitation Engineering*, vol. 24, no. 2, pp. 249–260, 2015.

[11] S. Chau, S. Aspelund, R. Mukherjee, M.-H. Lee, R. Ranganathan, and F. Kagerer, "A five degree-of-freedom body-machine interface for children with severe motor impairments," in *Proceedings of the International Conference on Intelligent Robots and Systems (IROS)*, 2017.

[12] R. Rupp, F. Biering-Sørensen, S. P. Burns, D. E. Graves, J. Guest, L. Jones, M. S. Read, G. M. Rodriguez, C. Schuld, K. E. Tansey-MD, K. Walden, and S. Kirshblum, "International Standards for Neurological Classification of Spinal Cord Injury: Revised 2019," *Topics in Spinal Cord Injury Rehabilitation*, vol. 27, no. 2, pp. 1–22, 2021.

[13] L. A. Harvey, G. Weber, R. Heriseanu, and J. L. Bowden, "The diagnostic accuracy of self-report for determining s4-5 sensory and motor function in people with spinal cord injury," *Spinal Cord*, vol. 50, no. 2, p. 119–122, 2012.

[14] N. A. Roman, R. S. Miclaus, C. Nicolau, and G. Sechel, "Customized manual muscle testing for post-stroke upper extremity assessment," *Brain Sciences*, vol. 12, no. 4, p. 457, 2022.

[15] A. Thompson, F. Rizzoglio, F. A. Neylon, D. R. Barsoum, L. E. Ammon, M. N. McCune, L. Miller, and B. Argall, "An evolution of assistive robot control to meet end-user ability," *Companion of the International Conference on Human-Robot Interaction (HRI)*, 2024.

[16] J. L. Patton, M. E. Stoykov, M. Kovic, and F. A. Mussa-Ivaldi, "Evaluation of robotic training forces that either enhance or reduce error in chronic hemiparetic stroke survivors," *Experimental Brain Research*, vol. 168, no. 3, pp. 368–383, 2006.

[17] N. Vaughan and B. Gabrys, "Comparing and combining time series trajectories using dynamic time warping," *Procedia Computer Science*, vol. 96, p. 465–474, 2016.

[18] W. Meert, K. Hendrickx, T. V. Craenendonck, H. B. Pieter Robberechts, and J. Davis., "DTAIDistance," 2022, DTAIDistance (Version v2). Zenodo. [Online]. Available: http://doi.org/10.5281/zenodo.5901139

[19] L. Aflatoony and S. Kolarić, "One size doesn't fit all: On the adaptable universal design of assistive technologies," *Proceedings of the Design Society*, vol. 2, p. 1209–1220, 2022.